Interfacial Rheology of Globular and Flexible Proteins at the Hexadecane/Water Interface: Comparison of Shear and Dilatation Deformation

Erik M. Freer,[†] Kang Sub Yim,[‡] Gerald G. Fuller,[‡] and Clayton J. Radke*,[†]

Chemical Engineering Department, University of California, Berkeley, California 94720-1462, and Chemical Engineering Department, Stanford University, Stanford, California 94305-5025

Received: October 25, 2003; In Final Form: December 16, 2003

After long-time exposure, protein adsorption at fluid/fluid interfaces is documented to produce interfacial, gellike networks. Formation of this network apparently results from adsorption-induced conformational changes and subsequent interprotein aggregation at the interface. We utilize interfacial shear and dilatational rheology to probe the structure of a globular protein, lysozyme, and a disordered protein, β-casein, and the kinetics of network formation at the hexadecane/water interface. For the first time, we present a detailed comparison of the interfacial shear and dilatational responses. For lysozyme, the shear moduli grow with interface age indicating a transition from fluidlike behavior at early times to network formation (solidlike behavior). Conversely, the interfacial shear moduli of β-casein change very little with interface age; in addition, both G' and G'' for β-casein are an order of magnitude smaller than those of lysozyme. The strong protein intramolecular interactions that stabilize the native conformation of lysozyme act as kinetic barriers to conformational change and later become strong intermolecular interactions upon partial unfolding at the interface. Hence, interprotein linkages form (i.e., aggregation into an interfacial gel), resulting in the growth of G' with time. We find that the interfacial dilatational storage modulus, E', is comprised of a static response and a dynamic response. The static response corresponds to a change in the surface pressure upon interfacial-area change and is strain-rate independent. The dynamic contribution corresponds to rearrangement and reconfiguration of the protein molecules within the interface and is analogous to the shear storage response (i.e., a measure of the strength of interprotein linkages). The magnitudes of E' and G' for lysozyme and β-casein suggest that lysozyme initially adsorbs in a state similar to its native conformation. The native rigidity of the protein is linked to its kinetic stability at the interface. Globular lysozyme, once adsorbed, resists compression giving a high dilatational storage modulus. Contrastingly, native β-casein lacks tertiary structure, resulting in a small interfacial dilatational storage modulus relative to lysozyme. With increasing interface age, the static modulus of β-casein changes insignificantly, whereas it decreases substantially for lysozyme, indicating partial unfolding and loss of intrinsic rigidity. Upon unfolding, interprotein linkages form through hydrophobic peptide−peptide interactions. Correspondingly, G' and the recoverable dilatational storage modulus, $\delta E'$, grow, signifying the onset of interfacial gelation.

Introduction

Dynamic mechanical properties of adsorbed protein films at fluid/fluid interfaces are of fundamental interest in understanding the rheology and stability of emulsions and foams.[1,2] Food emulsion and foam stability have been attributed to the formation of interfacial skins, as visualized from pendant drop (bubble) and thin-film studies.[3,4] Interfacial-skin formation is ascribed to a gellike network and is observed with a number of macromolecular surface-active species.[3,5−9] However, simple visual observation of interfacial skins provides little quantitative information on their formation kinetics, mechanical properties, or relaxation times. To overcome this ambiguity interfacial rheology, performed in the linear viscoelastic regime, is used here as a noninvasive technique to probe the structure of adsorbed protein films as a function of aging time.

Upon adsorption to a fluid/fluid interface, proteins partially unfold and rearrange within the interfacial region.[3,10−13] The structure of the adsorbed protein film and the adsorption kinetics are influenced by the stability of the native state.[3,14] For globular proteins, the dynamics of adsorption and conformation rearrangement in the interfacial region are extremely slow. In fact, the interfacial tension, interfacial concentration, and interfacial rheological properties continue to drift over time scales of days at both the air/water and oil/water interfaces.[3,12,14−18]

In this paper, we investigate how the structure of the adsorbed protein film changes with interface age at the oil/water interface using interfacial rheology. In addition, we study how the physicochemical properties of the protein affect interfacial dynamics. This is accomplished studying proteins that represent two extremes: lysozyme and β-casein. Lysozyme has a very stable, ordered ellipsoidal native structure, whereas β-casein configures almost randomly in solution.

In two-phase flows, an interfacial fluid element is generally subjected to both dilatation and shear deformation.[19] Several dilatational and shear apparatus exist to study the rheological properties of fluid interfaces.[19,20] The majority of dilatational studies focus on relatively small, reversibly adsorbed surfactant molecules where the dominating physics is transverse interfacial

* Author to whom correspondence should be addressed. Phone: 510-642-5204. Fax: 510−642−4778. E-mail: radke@cchem.berkeley.edu.
[†] University of California.
[‡] Stanford University.

10.1021/jp037236k CCC: $27.50
Published on Web 02/24/2004

transport (i.e., diffusion and sorption).[21,22] However, dilatational studies on insoluble monolayers and protein films clearly establish non-Newtonian behavior for macromolecules adsorbed at interfaces.[12,16,23−28] In contrast, interfacial shear studies have progressed much more slowly for simple surfactant systems, because great sensitivity is needed to measure the small forces.[29−34] However, shear techniques are suitable for macromolecular surface-active species that display substantial interfacial viscosity and viscoelastic behavior, which is observed in many protein systems.[12,16,18,27,35]

To our knowledge, only one previous study has compared the rheological response in both principal modes of deformation as a function of interface aging.[12] However, the rheological response in this study was not addressed over broad experimental time scales. Here, we investigate both the dilatational and shear responses over experimental time scales ranging from 20 s to 2 h using small-amplitude oscillatory flows and stress relaxation after a sudden strain. Our work gives new insight into the differences of the relaxation mechanisms that occur between the two principal modes of deformation and establishes a framework for interpretation of the viscoelastic properties of complex molecules at fluid/fluid interfaces.

Methods

Materials. Hen egg white lysozyme (Seikagaku Corp., Tokyo, Japan, Lot LF1121) and β-casein from bovine milk (Sigma Chemical Co., St. Louis, MO, Lot 30K7442) were used as received. Phosphate buffer solutions (100 mM; pH 7.0 ± 0.1) were made with distilled water further purified with a Milli-Q filtration unit (greater than 18.2 MΩ cm resistivity). Sodium phosphate dibasic heptahydrate and monobasic monohydrate were from EM Science (Gibbstown, NJ) and were of analytic grade. They were also used as received. Hexadecane (Mallinckrodt Baker, Inc., Paris, KY) was purified with use of a 12 in. long (0.5 in. i.d.) stratified column packed in the upper half with alumina from Fisher Scientific (Fair Law, NJ) and with silica gel from J.T. Baker (Phillipsburg, NY) in the lower half. The alumina and silica gels were activated at 400 °C for 12 h prior to use. Hexadecane was deemed acceptable only after the interfacial tension against the phosphate buffer solution remained constant at a value of 53.3 mN/m for 24 h. All experiments were conducted at 23 °C.

Interfacial Tension. To determine the dynamic interfacial tension of the hexadecane/water interface we used pendant-drop tensiometry. Details of this apparatus are given elsewhere.[8,36,37] The dynamic tension was followed in time by using axisymmetric drop-shape analysis.[38,39] Image acquisition and regression of the interfacial tension were performed with commercially available Dropimage software (Ramé-Hart, Inc.) by fitting the Laplace equation to the drop shape. Dropimage software also controlled an automatic pipetting system that maintained constant drop volume over the long time periods (1 day) over which dynamic tensions were measured. Typical precision in tension was ±0.5%. Results are later reported in terms of the dynamic surface pressure, π, which is defined as the difference between the clean oil/water tension (53.3 mN/m) and the tension with protein present.

Interfacial Dilatational Rheology. We measured the surface dilatational storage modulus, E', and the surface dilatational loss modulus, E'', by subjecting the oil/water interface to infinitesimal periodic area deformation. Additionally, we measured the interfacial dilatational relaxation modulus, $E(t)$, after a step-strain deformation.

Modification of the pendant-drop tensiometer enabled sinusoidal variations in the drop surface area.[40] Oscillation hardware consisted of a 50-mL gastight syringe mechanically coupled to a linear piezoelectric actuator from Physik Instrumente (Model P-840.3). Actuator motion was forced with a Hewlett-Packard function generator (Model 3325 A) that was computer controlled with National Instruments LabView software. The piezoelectric actuator was capable of subnanometer resolution ensuring the smoothest possible drop-volume oscillation. Further details of the oscillating-drop rheometer have been given elsewhere.[8,36,37]

We report the complex interfacial dilatational modulus, $E^*(\omega)$, which is defined as the linear proportionality factor between a periodically applied strain and the response stress

$$\bar{\gamma} e^{i(\omega t+\phi(\omega))} = E^*(\omega)\frac{\Delta A}{A_o} e^{i\omega t} \quad (1)$$

where A_o is the unperturbed oil-drop interfacial area, ΔA is the amplitude of interfacial area change, $\bar{\gamma}$ is the isotropic oil/water interfacial stress (measured from axisymmetric drop shape analysis), ω is the oscillation frequency, and ϕ is the phase angle difference between the applied strain and the response stress. The isotropic interfacial stress, $\bar{\gamma}$, is distinguished from the thermodynamic interfacial tension, γ, in that it generally includes nonequilibrium contributions.[19] Since the drop area oscillates periodically, the dilatational modulus exhibits two contributions: an elastic part accounting for the recoverable energy stored in the interface (storage modulus, E') and a viscous part accounting for energy lost through relaxation processes (loss modulus, E''). The interfacial storage and loss moduli correspond to the real and imaginary components of the complex dilatational elasticity: $E^* = E' + iE''$.

Interfacial moduli were followed over long time frames. To avoid continually oscillating the drops for such long periods, fresh drops were formed for each experiment and aged for the desired amount of time prior to imposing periodic oscillation. Equation 1 and equation 2 to follow demand small strains so that the interface lies in the linear viscoelastic regime. We set $|\Delta A/A_o|$ at 0.025, since nonlinear effects were observed above a relative strain of about 3.0%.

To determine the dilatational relaxation modulus, $E(t)$, we measured the stress relaxation after a sudden strain displacement. In these experiments, the interface was instantaneously deformed (expanded or compressed) and then held constant while the interfacial stress was measured (through axisymmetric drop shape analysis). The dilatational relaxation modulus was calculated as a function of time from the following expression

$$E(t) = \Delta\bar{\gamma}(t)\frac{A_o}{\Delta A} \quad (2)$$

where $\Delta\bar{\gamma}$ is the difference between the static tension prior to interfacial deformation and the measured isotropic interfacial stress. The dilatational relaxation modulus, $E(t)$, is related to the complex dilatational modulus, $E^*(\omega)$, via a Fourier transform.[41] The advantage of the step-strain technique is that the interfacial stress decays to a steady value within 2 h for the systems investigated in this work. Acquiring the same information with use of the oscillatory technique requires a very long time, because of the low frequencies needed to probe slow stress relaxation.

Interfacial Shear Rheology. To probe the interfacial shear rheology we used a recently developed interfacial stress rheometer, details of which are available elsewhere.[29] In this apparatus, a thin magnetized rod oscillates at the oil/water (or air/water) interface between two vertical glass walls. Rod motion was forced by an oscillating magnetic field. The position of

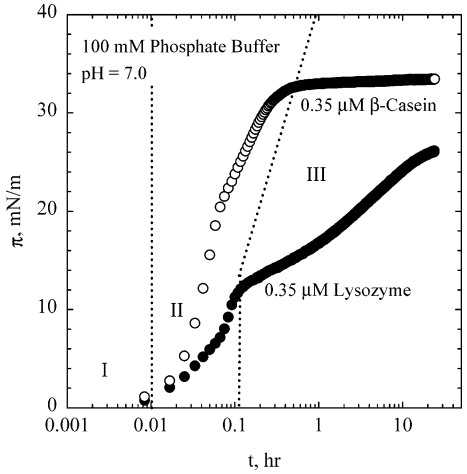

Figure 1. Dynamic surface pressures of lysozyme and β-casein. Dotted lines separate the three time regimes of surface-pressure change.

the rod was detected with an optical microscope and a photodiode array, allowing determination of the surface strain, ϵ, defined as the amplitude of the rod displacement divided by the distance between the rod and the vertical glass wall. For small periodic rod displacements, the complex interfacial shear modulus, $G^*(\omega)$, was ascertained as the linear proportionality constant between the applied stress and the response strain

$$\sigma e^{i(\omega t+\phi(\omega))} = G^*(\omega)\epsilon e^{i\omega t} \quad (3)$$

where σ is the interfacial shear stress and, again, $\phi(\omega)$ is the phase lag between the applied stress and measured strain response. Analogous to the complex dilatational modulus, the complex interfacial shear modulus is comprised of two contributions: $G^* = G' + iG''$, where the storage modulus, G', accounts for the recoverable energy stored in the interface and the loss modulus, G'', accounts for energy lost through shear dissipation processes.

Interfacial shear rheological behavior was also followed over long time frames. In addition, to ensure that these experiments were performed in the linear viscoelastic regime, ϵ was set at 0.02, since, again, above this relative strain, nonlinear effects were evident.

The interfacial shear and dilatational moduli were measured at a single frequency of 0.05 Hz, chosen because both protein films exhibit viscoelastic behavior on this experimental time scale. Additionally at this frequency, the duration of the experiment was short relative to the rate of surface-pressure change. Hence, the interfacial moduli do not change during the course of a rheologic measurement.

Results

Dynamic Surface Pressure. Dynamic surface pressures for lysozyme (5.0 mg/L) and β-casein (8.5 mg/L) at the same molar concentration, 0.35 μM, are shown in Figure 1 as closed and open circles, respectively, on a semilogarithmic scale. Three time regimes of tension lowering, commonly observed for many proteins,[3,14] are demarked by dotted lines. They include (I) induction, (II) monolayer saturation, and (III) interfacial gelation. In agreement with previously reported tension dynamics at the oil/water interface,[3,18] lysozyme shows an induction period that is of the same order of magnitude as that of β-casein. However, the long-time behavior is substantially different signifying important structural differences between the two proteins.

Lysozyme is a stable globular protein with significant α-helix and β-sheet structures. The molecular mass of lysozyme is 14.3 kDa; it has four disulfide bonds.[42] In addition, lysozyme possesses a very high isoelectric point (pI = 11.35), and the net valence at pH 7 is 9.[43] Conversely, the tertiary structure of β-casein is disordered with no disulfide bonds.[44] β-Casein is a larger molecule than lysozyme with a molecular mass of 24 kDa. The isoelectric point of β-casein is 4.6, and the net valence at pH 7 is -13.[43]

Following an initial rapid increase, the surface pressure of β-casein in Figure 1 changes little with continued interface aging. Lysozyme shows a similar surface-pressure increase after the induction period. However, the surface-pressure increase for β-casein after 1 h of interface aging is approximately double that observed for lysozyme. Apparently, the conformational freedom of the native β-casein molecule results in lower tensions and permits faster dynamics than for lysozyme.

In contrast to β-casein, the surface pressure of lysozyme continues to increase slowly over long times. The slope of the dynamic surface pressure is nonzero in Figure 1 even after 24 h of aging. Beverung et al.[3] observed similar dynamic surface pressures for numerous proteins at the heptane/water interface. Because many studies of proteins at interfaces focus on relatively short adsorption times (i.e., <24 h),[11,45−49] long-term aging effects are not taken into account.

Beverung et al.[3] attributed the long-time tension behavior to interfacial gellike structures forming. They visually observed interfacial skins (film collapse) upon compression of the interface. In the present study, the interface was compressed after 12 h of aging by decreasing the drop volume at a constant rate of 5 mL/s. Film collapse was observed for both lysozyme and β-casein. However, collapse occurred after an 80% drop-volume reduction for β-casein versus a 40% volume reduction for lysozyme, suggesting that lysozyme forms a more robust interfacial network.

Irreversible Adsorption. It is well-known that proteins exhibit irreversible adsorption at fluid/fluid interfaces depending on the protein type, protein concentration, and the interface aging time.[14,17,50−52] Additionally, stable Langmuir protein monolayers are commonly formed at the air/water interface[53−58] suggesting irreversible adsorption. We utilize continuous flow tensiometry (CFT)[50] to investigate irreversible adsorption of lysozyme and β-casein at the hexadecane/water interface. After aging the interface for 12 h, 20 cell volumes of protein-free buffer solution (surface tension 72 mN/m) were flushed through the optical cuvette, resulting in a negligible bulk protein concentration. Following washout, stirring was stopped, and the tension was monitored over time for an additional 12 h. A typical result is shown in Figure 2 for lysozyme. Three time regimes separated by dashed lines are labeled in the figure. These regimes include (1) adsorption, (2) washout, and (3) continued aging after complete depletion of protein from the bulk aqueous solution. Scatter in the surface pressures observed during washout is an artifact of drop vibration due to stirring of the cell contents.[50] There is a break along the abscissa shown to emphasize the long aging period. An approximate 2 mN/m rise in the surface pressure for lysozyme is observed after washout: a 10% change. Thus, some small amount of lysozyme is reversibly adsorbed, but the small decrease in the surface pressure upon washout indicates that most all of the protein is irreversibly adsorbed on the time scale of investigation (i.e. the surface concentration of irreversibly adsorbed protein is high enough to result in a surface pressure of 19 mN/m).[52] Although the results for β-casein are not shown, the same washout experiment was

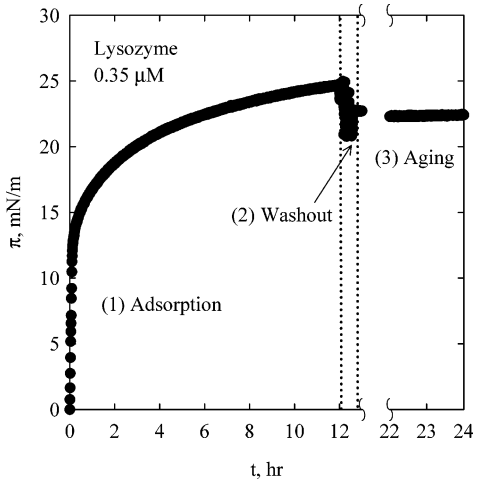

Figure 2. Loading and washout of lysozyme at the hexadecane/water interface. Phosphate buffer (100 mM), pH 7.0.

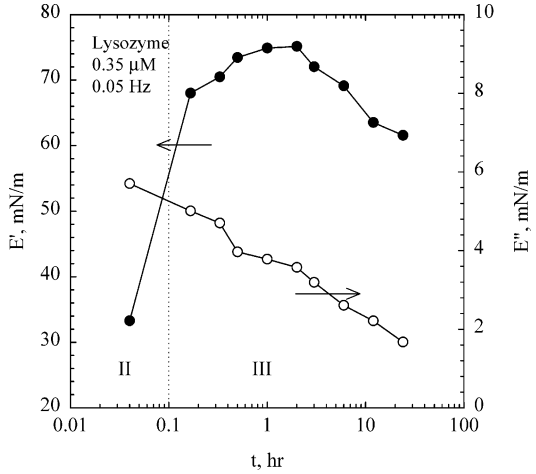

Figure 3. Dilatational response versus interface aging time for 0.35 μM (5.0 mg/L) lysozyme at the hexadecane/water interface. Phosphate buffer (100 mM); pH 7.0. A vertical dotted line separates the time regimes of surface-pressure change.

performed yielding an approximate 3 mN/m rise in tension following 12 h of adsorption at the interface. Hence, β-casein is also irreversibly adsorbed after 12 h of interface exposure. Thus, as opposed to assuming reversible adsorption,[59,60] we are obliged to incorporate irreversibility into our description of protein adsorption.

The starkly different collapse films observed for β-casein and lysozyme suggest that other factors, in addition to irreversible adsorption, contribute to network (skin) formation. We use interfacial rheology in the linear-response regime to characterize the interfacial films.

Interfacial Rheology: Small-Amplitude Oscillatory Flows. Figures 3 and 4 show the two dilatational and shear moduli for lysozyme on semilogarithmic scales for an oscillation frequency of 0.05 Hz. Lines in these figures guide the eye. A vertical dashed line separates the monolayer saturation and interfacial gelation: Regimes II and III, respectively. For both dilatation and shear, the first data points are measured well after the induction period and near the end of monolayer saturation (i.e. Regime II of Figure 1). The dilatational storage modulus for lysozyme in Figure 3 is approximately an order of magnitude larger than the loss modulus at all aging times (note the scale change between the left and right ordinates), suggesting that the interface is primarily elastic. In contrast, Figure 4 reveals

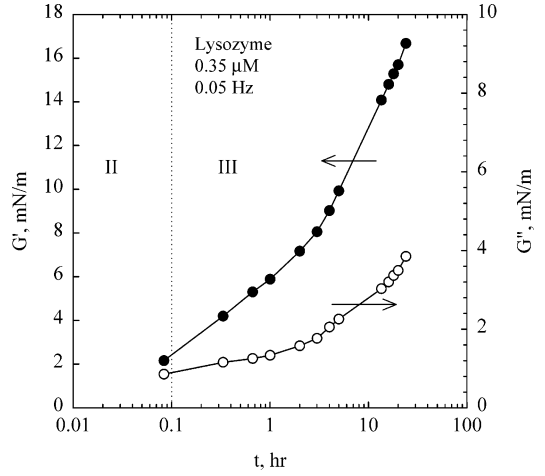

Figure 4. Shear response versus interface aging time for 0.35 μM (5.0 mg/L) lysozyme at the hexadecane/water interface. Phosphate buffer (100 mM); pH 7.0. A vertical dotted line separates the time regimes of surface-pressure change.

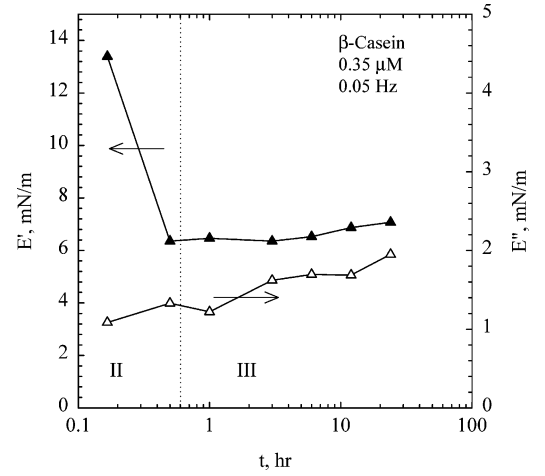

Figure 5. Dilatational response versus interface aging time for 0.35 μM (8.5 mg/L) β-casein at the hexadecane/water interface. Phosphate buffer (100 mM); pH 7.0. A vertical dotted line separates the time regimes of surface-pressure change.

that the shear storage moduli for lysozyme are only modestly larger than the loss moduli at early time (in Regime II).

As aging progresses into Regime III, the dilatational storage modulus increases, reaches a maximum at 2 h, and then decreases. Conversely, the dilatational loss modulus decreases monotonically with time. The observed late-time decrease in the dilatational storage modulus is somewhat unexpected, because skin formation is many times associated with a slow continued increase in the dilatational storage modulus.[8,61] For globular proteins, however, similar decreases in the dilatational storage modulus with increasing surface pressure or aging time have been reported at both the oil/water and air/water interfaces.[14,26,45] Conversely, both shear moduli in Figure 4 increase with time. As with the dilatational moduli, the shear storage modulus is an order of magnitude larger than the shear loss modulus after 24 h of aging.

Companion interfacial dilatation and shear moduli for β-casein are shown in Figures 5 and 6, respectively, as a function of interface aging time on semilogarithmic scales for an oscillation frequency of 0.05 Hz. Again, the lines in the figures guide the eye, and Regimes II and III are demarked. As noted earlier, the interfacial dynamics of β-casein at the hexadecane/water interface are much more rapid than for lysozyme; the interfacial-

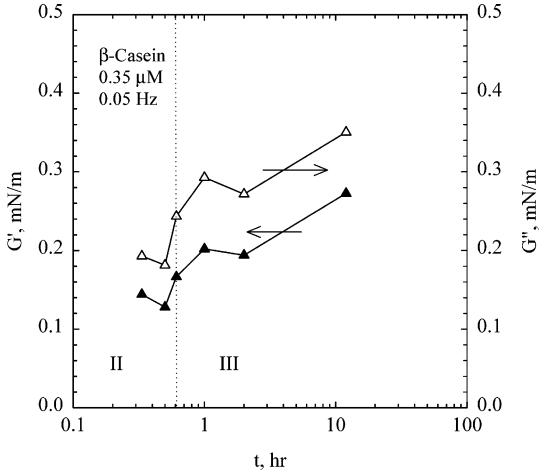

Figure 6. Shear response versus interface aging time for 0.35 μM (8.5 mg/L) β-casein at the hexadecane/water interface. Phosphate buffer (100 mM); pH 7.0. A vertical dotted line separates the time regimes of surface-pressure change.

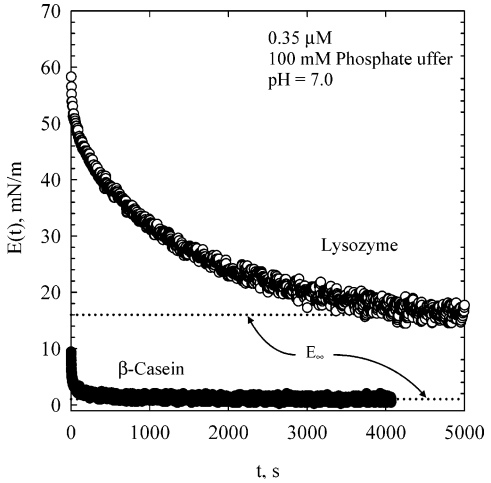

Figure 7. Dilatational response for lysozyme (open circles) and β-casein (closed circles) after a step compression of the interfacial area ($|\Delta A/A_o| = 0.025$). The interface was aged for 24 h before compression. Phosphate buffer (100 mM); pH 7.0. The static modulus E_∞ is labeled.

gelation regime appears to be substantially less pronounced than that for lysozyme. Importantly, the dilatational and shear moduli for β-casein are both an order of magnitude smaller than those for lysozyme.

Similar to lysozyme, the dilatational storage modulus of β-casein in Figure 5 decreases with interface age, but at a much earlier time already starting in Regime II. After the initial decrease, the storage modulus in Regime III increases very slightly in time, but the loss modulus, which is the same order of magnitude as the storage modulus, approximately doubles. The relative magnitudes of the storage and loss moduli suggest that the interfacial layer is fluidlike. This finding is confirmed by the interfacial shear moduli shown in Figure 6. Here, the shear loss modulus is larger than the storage modulus. Both are an order of magnitude smaller than the corresponding dilatational moduli in Figure 5.

The dilatational and shear moduli reported in Figures 3−6 are comprised of all response modes that have relaxation times greater than the time scale of investigation (i.e., here 0.05 Hz).[41] To determine the number of relaxation modes and the contribution of each mode, we measure the dilatation relaxation modulus, $E(t)$, as a function of relaxation time (equivalent to measuring E^* as a function of frequency). By considering a larger time interval in the relaxation spectrum, we separate different modes that contribute to the measured E'.

Interfacial Rheology: Stress Relaxation. As a second rheological probe, we measure the relaxation of the interfacial tension after the drop area is suddenly compressed and calculate the dilatational elasticity using eq 2 as outlined above. A caveat of the stress-relaxation technique, as applied to our systems, is that the structure of the interface layer must not age appreciably during the course of the relaxation experiment (quasiequilibrium). This condition is fulfilled when the interfacial-stress change due to compression is much faster than the interfacial-tension change due to aging (i.e., the slow surface pressure changes seen in Figure 1). Figure 7 displays the dilatational relaxation modulus, $E(t)$ ($|\Delta A/A_o| = 0.025$), for lysozyme and β-casein as open and closed circles, respectively, after aging the interface for 24 h. For both lysozyme and β-casein, the modulus decays to a nonzero value denoted by E_∞ in Figure 7, where the subscript, ∞, indicates the zero-frequency limit (i.e., $t \rightarrow \infty$). Hence, the interfacial tension after relaxation is not the same as the initial value. Further, the dilatational relaxation modulus, $E(t)$, of lysozyme is an order of magnitude larger than

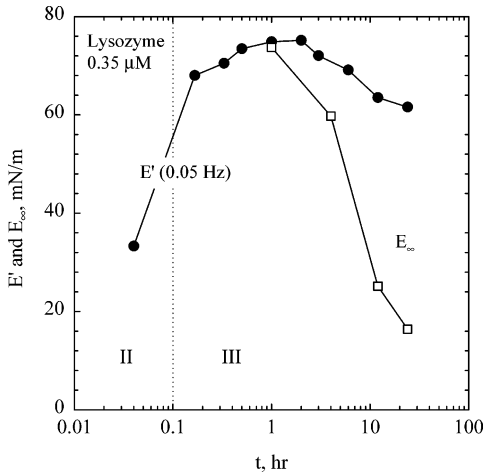

Figure 8. Dilatational storage modulus, E', at an oscillation frequency of 0.05 Hz and the static modulus, E_∞, versus interface aging time for 0.35 μM (5.0 mg/L) lysozyme at the hexadecane/water interface. Phosphate buffer (100 mM); pH 7.0. A vertical dotted line separates the time regimes of surface-pressure change.

that of β-casein. This finding is consistent with the interfacial dilatational and shear moduli in Figures 3−6.

The static dilatational modulus, E_∞, arises from an interfacial-tension change with an interfacial-area change at constant adsorbed amount. Accordingly, the static modulus is given by the slope of the surface pressure−area isotherm according to the Gibbs elasticity: $E_G = -d\pi/d \ln A$.[19] In our protein experiments, E_∞ is not strictly an equilibrium Gibbs elasticity since the conformation of the adsorbed molecules changes with time as the interface slowly ages. Nevertheless, similar to the surface pressure−area isotherms of insoluble surfactant monolayers, the static modulus can be used to characterize the structure of the adsorbed layer.[62]

Figure 8 contrasts the dilatational storage modulus, E', and the static dilatational relaxation modulus, E_∞, for lysozyme versus interface aging time on a semilogarithmic scale. Solid lines guide the eye. The first datum for the static modulus is reported after 1 h of aging, because, before this time, the interfacial tension changes too quickly to permit measurement of the dilatational relaxation modulus. After 1 h of interface

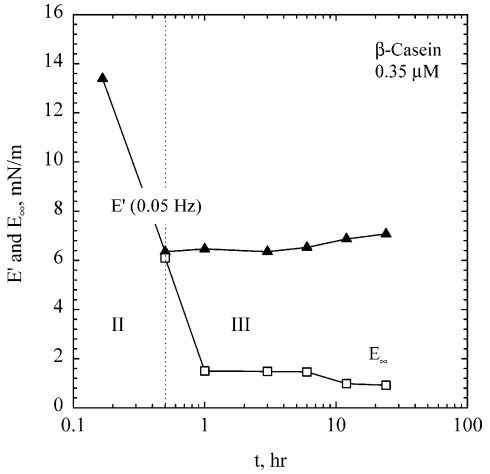

Figure 9. Dilatational storage and static modulus versus interface aging time for β-casein at the hexadecane/water interface. Phosphate buffer (100 mM); pH 7.0. A vertical dotted line separates the time regimes of surface-pressure change.

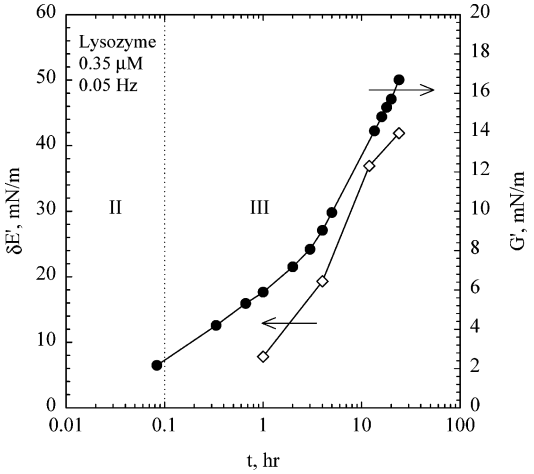

Figure 10. Dilatational recoverable stress, $\delta E'$, at an oscillation frequency of 0.05 Hz and the shear storage modulus versus interface aging time for 0.35 μM (5.0 mg/L) lysozyme at the hexadecane/water interface. Phosphate buffer (100 mM); pH 7.0. A vertical dotted line separates the time regimes of surface-pressure change.

aging, E' and E_∞ are practically identical, but as aging progresses, E_∞ declines rapidly and the difference becomes pronounced.

Likewise for β-casein, the dilatational static relaxation modulus and dilatational storage modulus versus aging time are compared in Figure 9. The first datum for the static modulus is now measured after 0.5 h of aging. Here, similar to the storage modulus, the static modulus changes very little at interface aging times greater than 1 h.

Gardner et al.[63] argue that for insoluble surfactant monolayers the interfacial stress upon a dilatational deformation is composed of both a static value and a dynamic contribution, which has been verified experimentally.[23,24] To separate the dynamic contribution to E' at a given frequency from the static contribution, E_∞, we define a recoverable dilatational storage modulus: $\delta E' \equiv E' - E_\infty$.

A fascinating correspondence between $\delta E'$ and G' is highlighted in Figures 10 and 11. Figure 10 shows the recoverable dilatational storage modulus and the shear storage modulus for lysozyme on a semilogarithmic scale versus interface aging time at a frequency of 0.05 Hz. The recoverable dilatational storage modulus and shear storage modulus for

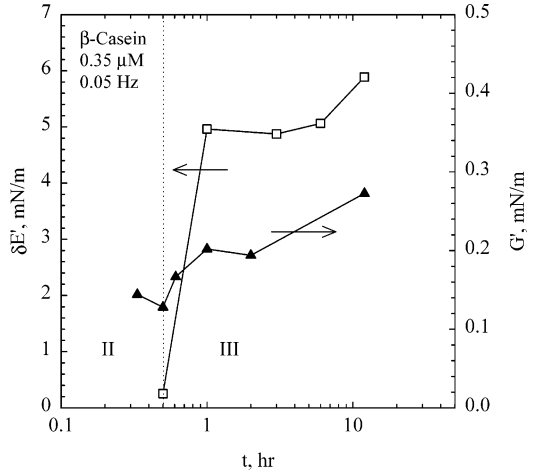

Figure 11. Dilatational recoverable stress and shear storage modulus versus interface aging time for 0.35 μM (8.5 mg/L) β-casein at the hexadecane/water interface. Phosphate buffer (100 mM); pH 7.0. A vertical dotted line separates the time regimes of surface-pressure change.

lysozyme show identical aging trends, but $\delta E'$ is approximately double that of G'. Figure 11 shows the companion recoverable dilatational storage modulus and shear storage modulus for β-casein versus interface aging time. After 1 h of interface aging, $\delta E'$ again grows at a rate similar to that observed for G'. Here, however, the recoverable dilatational storage modulus is an order of magnitude greater than the shear storage modulus. Importantly, both the recoverable dilatational storage modulus and the shear storage modulus of lysozyme are an order of magnitude greater than those of β-casein consistent with the visual observation of interfacial skins noted earlier. To our knowledge, Figures 10 and 11 are the first experimental results demonstrating a connection between the interfacial dilatational and shear moduli.

Discussion

To understand the measured interfacial rheology of lysozyme and β-casein we illustrate schematically the adsorption process of proteins at fluid/fluid interfaces in Figure 12 corresponding to the three time regimes of tension lowering demonstrated in Figure 1.[3] In Figure 12a, bulk protein molecules in their native globular conformation initially adsorb onto the interface in a conformation resembling the native state (Regime I). Tension lowering in this regime is minimal.[3] As time progresses and the interfacial concentration of protein increases, adsorbed protein molecules slowly reconfigure, as illustrated pictorially in Figure 12b (Regime II). Here the hydrophobic residues of the adsorbed protein are partially exposed and interact with the oil phase (loops and trains)[10] and with other exposed peptide residues of nearby proteins (interprotein aggregation). Irreversible adsorption develops.[10] Continued adsorption and conformational changes occur at later times, as illustrated in Figure 12c (Regime III). Aggregation into a network is extensive in Regime III resulting in interfacial-skin formation that has been coined interfacial gelation.[3,12,14] As shown in Figure 12c, it is also likely that multilayers form in this long-time regime.

The adsorption mechanism described in Figure 12 is general for globular proteins with the caveat that the structure of the interface diagrammed in Figure 12a−c may be the terminal or a kinetically limited state relative to the time scale of experimental investigation. Energy barriers to conformational rearrangement make the states described in parts a and b of Figure

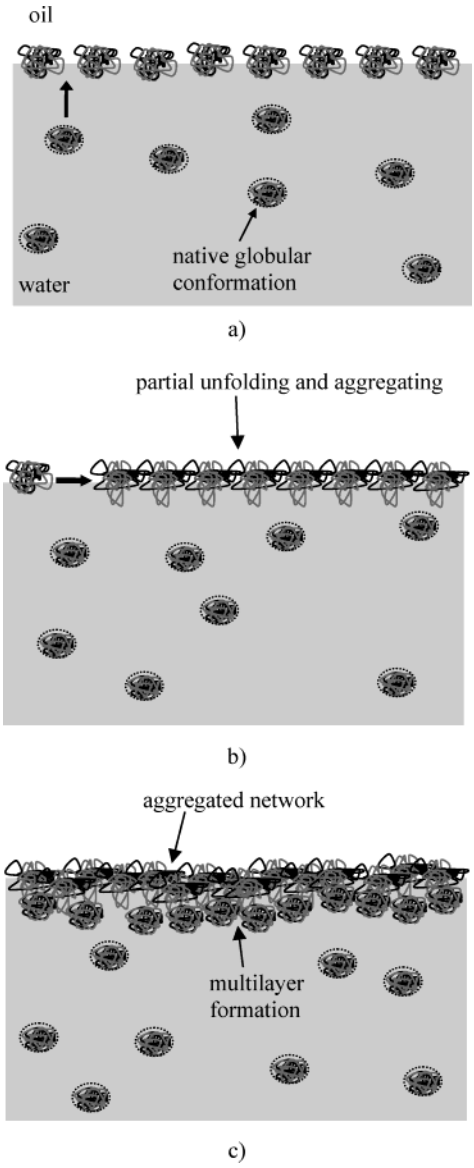

Figure 12. Adsorption mechanisms for proteins at fluid/fluid interfaces. (a) Initial adsorption in a conformation resembling the native state. (b) Upon further adsorption and interface aging the proteins partially unfold exposing hydrophobic groups. (c) Proteins continue to unfold and aggregate, and multilayers form. A network or glassy state develops after continued aging.

12 kinetic intermediates. Even at the same interfacial concentration, Γ, the nativelike (globular) and partially unraveled aggregated states give rise to substantially different interfacial rheological properties. Hence, both Γ and the protein conformation (i.e., the aging time) are needed to characterize the interface.[64] Figure 12 emphasizes the strong role of interface aging in protein adsorption.

Lysozyme. Even under diffusion control, adsorption of lysozyme at the oil/water interface is relatively rapid at early times (i.e., less than 0.01 h in Regime I of Figure 1). The almost zero surface pressures seen in this time regime are likely due to the large size of protein molecules. For example, we calculate less than a 0.5 mN/m surface pressure increase for 50% monolayer coverage of lysozyme in the globular state ($1/\Gamma_{max}$ = 2000 Å^2/molecule).[3] At this stage, the adsorbed protein molecules remain close to their native structure and interact very little with each other. This assertion can be argued by extrapolating the dilatational and shear moduli in Figures 3 and 4 to zero interface aging. Because a clean interface (protein-free) does not exhibit a rheological response, the dilatational and shear moduli in Figures 3 and 4 increase from zero at t = 0 to the first reported experimental value. At 0.01 h, lysozyme exerts values of less than 1 mN/m for both G' and G'', confirming that the interprotein interactions for the nativelike conformation of lysozyme are not strong at the interface.[12,27,65] This finding suggests that the corresponding E' values in Figure 3 are dominated by the compressibility of reversibly adsorbed noninteracting protein molecules (i.e., the Gibbs elasticity: $E_G = d\pi/d \ln \Gamma$). The initially high datum of E'' in Figure 3 compared to that of G'' in Figure 4 also may result from a fraction of reversibly adsorbed protein in Regime I. In this case, the dominant contribution to E'' is diffusion dissipation as captured, for example, in the diffusion exchange model of Lucassen and Van den Temple,[22] not viscous dissipation. The (extrapolated) rise in E' in Regime I is explained by increasing adsorption with time.

Regime II in Figure 12b is characterized by more densely packed adsorbed protein molecules. With increased exposure time to the interface and with increased adsorption amount, the protein molecules begin to unfold[10] and interact within the interfacial region. At this point, the dynamics are dominated by the kinetics of conformation change and irreversible adsorption due to unfolding, aggregation, and rearrangement of sublayer protein molecules (in order to incorporate into the adsorbed layer). These processes are signified experimentally by the rise in the dynamic surface pressure and by the shear storage and loss moduli of lysozyme in Figures 1 and 4, respectively.

The relatively low magnitude of the shear storage moduli in Regime II indicates that the interface is not yet strongly elastic. We explain the rapid increase in the dilatational storage modulus in Figure 3 around 0.1 h as due to increased adsorption raising the Gibbs elasticity of a primarily irreversibly adsorbed protein layer (i.e., in analogy to the static dilatational elasticity of insoluble surfactant monolayers[24,25]). Concomitant with the falling fraction of reversibly adsorbed proteins in Regime II, the dilatational loss modulus declines. Nevertheless, the large values of E' that appear in Region II of Figure 3 imply that lysozyme still retains much of its native conformation. The reason is as follows. The static Gibbs component of the irreversibly adsorbed protein layer is comprised of two components: (1) an interprotein contribution (aggregation) and (2) an intraprotein contribution (intrinsic flexibility of the partially unfolded structure).[14] For hard globular proteins, like lysozyme, intraprotein interactions dominate, yielding large values for E' (i.e., the hard nativelike protein resists compression when squeezed).[14,26,45,64] In fact, an order of magnitude difference in E' has been observed upon adsorption for the same protein with different bulk conformations: globular and flexible.[14] Conversely, in this same time period, both G' and G'' remain modest, characteristic of fluidlike behavior.[29,66]

Regime III is shown in Figure 12c and begins between 0.1 and 0.2 h of interface aging for lysozyme (cf., Figure 1). This regime is a continuation of the process of unfolding and aggregation started in Regime II. However, later in Regime III aggregated multilayers may also form.[67] The onset of Regime III is marked by an appreciable growth in G' relative to G'' as shown in Figure 4. This observation is consistent with visual interfacial-skin formation upon interface compression and suggests that aggregated proteins form junctions that can be relatively long-lived resulting in a time-average percolating network (a physical gel or a glassy film).[16,58,68]

In the dilatational mode of deformation, the picture changes

slightly. Dilatational deformation alters the adsorption density in the interface resulting in a static elasticity for the irreversibly attached proteins. Hence, a significant difference between the aging behavior of the dilatational and shear moduli is clearly observed in Figures 3 and 4. The shear moduli increase at long interface aging times (> 2 h) in contrast to the decreasing dilatational response. As described below, both responses are consistent with the picture of an interfacial network (physical gel or glassy film).

The shear moduli increase due to the continued unfolding and to the increasing number of interprotein peptide−peptide junctions (aggregation).[12,27] The resulting interfacial network is primarily elastic on the experimental time scale of 0.05 Hz in Regime III, as indicated by the larger values of G' compared to those of G''. The network of adsorbed lysozyme protein appears to continue building in strength over very long time periods (up to a day in Figure 4).

Conversely, the dilatational static Gibbs elasticity of the irreversibly adsorbed protein layer is comprised of two components: intra- and intermolecular. It is the intrinsic intramolecular flexibility of the individual adsorbed protein molecules that apparently gives rise to the decline of the dilatational storage modulus of lysozyme reported Figure 3. As unfolding continues in Regime III, the original hard native structure softens, and E' falls. De Feijter and Benjamins[69] and, more recently, Fainerman et al.[70] argue for a decline in the static Gibbs modulus due to a size decrease of a compressible adsorbed molecule as the surface pressure increases. Our argument for adsorbed lysozyme is somewhat similar except that the origin is from kinetic-limited conformation change to produce progressively more flexible adsorbed protein molecules. For exactly the same reason, E_∞ strongly decreases with aging time, as evident in Figure 8. The dilatational loss modulus in Figure 3 also diminishes with time during Regime III, because interprotein connections continue to form that increase the relaxation time and result in more solidlike behavior.

In Figure 8, E_∞ decreases at a faster rate than does E' giving rise to the recoverable dilatational storage modulus, $\delta E'$ (i.e., the dynamic contribution to the dilatational storage modulus). As the protein molecules progressively unfold, intermolecular aggregation and network formation commences giving rise to slow relaxation and a finite G' (as previously discussed). Analogously, $\delta E'$ arises from rearrangement and reconfiguration of the adsorbed proteins and is the dilatational counterpart of G'. This point is emphasized in Figure 10, showing the similarity between $\delta E'$ and G' with interface aging. Thus, the growth of $\delta E'$ with aging time also reflects formation of an interfacial skin. Consequently, the trends in Figure 3, 4, 8, and 10 are all consistent with the picture of lysozyme adsorption illustrated in Figure 12.

***β*-Casein.** The general picture of protein adsorption and interfacial rheology for the globular protein lysozyme also applies for the flexible protein β-casein. Now, however, the random-coil structure of native β-casein makes conformational changes at the interface much faster. Further, intraprotein interactions are much weaker in β-casein than those for lysozyme.

In Figure 1, the lag period preceding the transition to Regime II (0.01 h) is the same for β-casein and lysozyme. Similar to lysozyme, we argue that the initially low surface pressure of β-casein results from the large size of adsorbed protein molecules and from the paucity of intermolecular interactions. Extrapolation of G' and G'' to zero time in Figure 6 again confirms that the protein molecules interact minimally in Regime I.

The transition to Regime II spanning times between 0.01 and 0.5 h is accompanied by a marked increase in the surface pressure. Unlike lysozyme, nearly the entire surface-pressure change in Figure 1 occurs in Regime II. β-Casein shear moduli in Regime II of Figure 6 are strikingly smaller than the corresponding values for lysozyme in Figure 4. Also, G'' is larger than G' of β-casein suggesting some interprotein interactions, but the interface remains soft and primarily fluidlike. The shear moduli change very little relative to the surface pressure in this time regime.

In contrast to the shear moduli in Regime II, E' decreases for β-casein in Figure 5 suggesting a maximum value very early on in the adsorption process. Because of rapid adsorption of the random-coil protein, this maximum is not measurable with our equipment. The relative magnitudes of G' and E' for β-casein suggest that E' is dominated by the static Gibbs component of the irreversibly adsorbed proteins. We argue that the decrease in E' results from a later-time size decrease of the adsorbed molecule as the surface pressure increases as proposed by De Feijter and Benjamins.[69] This is because β-casein is already quite flexible in the native state and does not soften much further upon reconfiguration at the interface. Surface pressure−interfacial concentration isotherms measured at the oil/water and air/water interfaces for β-casein indeed confirm that the static modulus passes through a maximum with increasing adsorption, Γ.[52] Our findings at the oil/water interface agree qualitatively with β-casein adsorption at the air/water interface.[11,14−16,26,52−57,67,71] Comparison between the kinetics of rheological property change of β-casein and lysozyme in Regime II (cf. Figures 3−6) shows a strong connection to native protein stability. The shift in the maximum of E' to an earlier time relative to lysozyme is likely due to the inherent flexibility of β-casein and the concomitant absence of kinetic barriers to conformational change.[15] We argue that the lack of tertiary structure because of weak peptide−peptide interactions for native β-casein results in rapid adsorption kinetics, as detected by E^*, G^*, and π.

Regime III occurs at approximately 0.5 h of interface aging for β-casein; the subsequent change in surface pressure is minor in Figure 1. This contrasts with the long-time structure evolution observed for lysozyme. In Figure 6, G' and G'' increase very slightly with interface age in Regime III. Similarly, E' and E'' increase with interface aging in Regime III but, again, only slightly, as illustrated in Figure 5. The growth rate of E'' is higher than that for E' in Figure 5, opposite to the trend observed in the shear moduli. It is likely that multilayers form in this regime[44] and that subsequent adsorbed layers may be reversibly adsorbed.[52] For this multilayer interfacial structure, exchange of the reversibly adsorbed proteins with the bulk aqueous phase perhaps explains continued growth of E'' through diffusion dissipation.

As shown in Figure 9, the static component of the dilatational modulus, E_∞, for β-casein initially decreases and then changes only slightly after 1 h of interface aging. Conformational rearrangements that occur upon adsorption are not strongly kinetically limited as observed for lysozyme. The small magnitude of E_∞ compared to that of lysozyme suggests that at this interfacial concentration the protein is compressible and soft. From Figure 11 in Regime III, there is little change in $\delta E'$ consistent with the observed changes in the shear moduli for β-casein. The small growth likely results from increased

adsorption and multilayer formation, similar to the picture in Figure 12c.

Our rheological studies of lysozyme and β-casein indicate that dilatation and shear deformation probe different molecular properties of the interface. Shear deformation is apparently sensitive to the intermolecular interactions between the adsorbed proteins (aggregation). Because no area changes are imposed during shear, the hardness or softness of the primary protein particles that comprise the aggregated structure are not probed. Conversely, dilatation deformation invokes interface area change. Hence, dilatational deformation detects the intrinsic softness or hardness of the protein as it unfolds and reconfigures at the interface, in addition to the interprotein interactions and irreversible adsorption (relative to the experimental time scale). Rheological parameters from dilatation are, therefore, more revealing of interfacial structure, but at the same time are more difficult to interpret. The dilatational storage modulus is composed of both a static and a dynamic contribution. Thus, in dilatational deformation, the storage relaxation response can be decomposed into E_∞ (static) and $\delta E'$ (dynamic) components. E_∞ characterizes the molecular structure of the interface for irreversibly adsorbed molecules through the Gibbs elasticity. The dynamic contribution, $\delta E'$, is the dilatational counterpart of G' for irreversibly adsorbed molecules. An important difference between E_∞ and $\delta E'$ is that E_∞ is a material constant of the interface not changing as a function of strain rate (oscillation frequency). We note in this work that a single fixed oscillation frequency of 0.05 Hz was investigated. Examination of the frequency response of the shear and dilatational moduli is warranted.

Conclusions

The constitutive behavior of lysozyme and β-casein adsorbed at the oil/water interface in both shear and dilatational deformation is viscoelastic with interfacial moduli that change significantly with aging. Lysozyme and β-casein are structurally very different proteins. Lysozyme is a stable, globular (hard) protein, whereas β-casein has a flexible (soft) random configuration. We are thus able to probe the kinetics of adsorption, conformational change, and intermolecular aggregation at the oil/water interface for proteins that represent extremes with respect to their native state stability.

Lysozyme and β-casein exhibit three time regimes of interfacial tension lowering: (I) induction, (II) monolayer saturation, and (III) interfacial gelation. In Regime I, there is negligible surface-pressure change and little intermolecular interaction for both proteins. In Regime II, both proteins exhibit a substantial surface-pressure increase, but for β-casein nearly the entire surface-pressure change occurs. The rapid kinetics of β-casein adsorption relative to lysozyme is due to its soft flexible structure. At later times, a slow continued drift in the surface pressure signifies the onset of interfacial gelation (Regime III). Here both proteins are irreversibly adsorbed at the oil/water interface. This regime is much more pronounced for lysozyme than for β-casein, and film collapse upon drop area compression (visual observation of skins) suggests that lysozyme forms a more robust and longer lived physical network.

Both interfacial shear and dilatational moduli probe the structure of the adsorbed protein layer. For lysozyme, the shear moduli grow with interface age showing a transition from fluidlike behavior at early times (Regimes I and II) to network formation with increased interface aging (solidlike behavior) in Regime III. Conversely, the shear moduli of β-casein change very little with interface age; in addition, G' and G'' of β-casein are an order of magnitude smaller than those of lysozyme. These differences reflect how the stability of the native state influences the kinetics and magnitudes observed for G' and G''. Apparently, the strong protein intramolecular interactions that stabilize the native conformation of lysozyme later become strong intermolecular interactions upon interface-induced unfolding. Hence, interprotein linkages form (e.g., aggregation into an interfacial gel), resulting in growth of G'.

We show that the interfacial dilatational storage modulus is comprised of two components: (1) a static response and (2) a dynamic response. The static response corresponds to a change in the surface pressure with interfacial-area change and is independent of rate of strain. The static response is characteristic of irreversibly adsorbed surface-active molecules, similar to the Gibbs elasticity of insoluble monolayers. The dynamic contribution corresponds to rearrangement and reconfiguration of molecules within the interface and is analogous to the shear storage response (i.e. a measure of the strength of interprotein linkages). Therefore, G' and $\delta E'$ for irreversibly adsorbed molecules measure the same relaxation processes. Conversely, for reversibly adsorbed molecules, diffusion dissipation may dominate the dilatational response.

From the measured magnitudes of E' and G' for lysozyme and β-casein, it appears that lysozyme initially adsorbs in a state similar to its native conformation. The rigidity of the protein is linked to its stability at the interface. For lysozyme, once adsorbed, the hard protein resists compression giving a high dilatational modulus. Contrastingly, β-casein lacks tertiary structure making the native protein soft. This softness is observed in the small magnitude of the dilatational modulus relative to lysozyme in Regime II. With increasing interface aging (Regime III), the static modulus of β-casein changes insignificantly, whereas it decreases substantially for lysozyme indicating loss of intrinsic rigidity and partial unfolding. Upon unfolding, protein linkages form through hydrophobic moieties, and G' and $\delta E'$ grow in time, signifying interfacial gelation. Thus, this study emphasizes the utility of interfacial rheology in probing the structure of adsorbed macromolecules and the kinetics of interfacial structure change.

References and Notes

(1) Murray, B. S.; Cattin, B.; Schuler, E.; Sonmez, Z. O. *Langmuir* **2002**, *18*, 9476−9484.
(2) Borbas, R.; Murray, B. S.; Kiss, E. *Colloid Surf. A* **2003**, *213*, 93−103.
(3) Beverung, C. J.; Radke, C. J.; Blanch, H. W. *Biophys. Chem.* **1999**, *81*, 59−80.
(4) Pereira, L. G. C.; Johansson, C.; Blanch, H. W.; Radke, C. J. *Colloid Surf. A* **2001**, *186*, 103−111.
(5) Mackie, A. R.; Gunning, A. P.; Ridout, M. J.; Morris, V. J. *Biopolymers* **1998**, *46*, 245−252.
(6) Petkov, J. T.; Gurkov, T. D.; Campbell, B. E.; Borwankar, R. P. *Langmuir* **2000**, *16*, 3703−3711.
(7) Wijmans, C. M.; Dickinson, E. *Langmuir* **1998**, *14*, 7278−7286.
(8) Freer, E. M.; Svitova, T. F.; Radke, C. J. *J. Pet. Sci. Eng.* **2003**, *39*, 137.
(9) Reisberg, J.; Doscher, T. M. *Prod. Mon.* **1956**, *21*, 43.
(10) Anderson, R. E.; Pande, V. S.; Radke, C. J. *J. Chem. Phys.* **2000**, *112*, 9167−9185.
(11) Graham, D. E.; Phillips, M. C. *J. Colloid Interface Sci.* **1979**, *70*, 403−414.
(12) Benjamins, J.; Vader, F. V. *Colloids Surf.* **1992**, *65*, 161−174.
(13) Rao, C. S.; Damodaran, S. *Langmuir* **2000**, *16*, 9468−9477.
(14) Pereira, L. G. C.; Theodoly, O.; Blanch, H. W.; Radke, C. J. *Langmuir* **2003**, *19*, 2349−2356.
(15) Atkinson, P. J.; Dickinson, E.; Horne, D. S.; Richardson, R. M. *J. Chem. Soc., Faraday Trans.* **1995**, *91*, 2847−2854.
(16) Bantchev, G. B.; Schwartz, D. K. *Langmuir* **2003**, *19*, 2673−2682.

(17) Tupy, M. J.; Blanch, H. W.; Radke, C. J. *Ind. Eng. Chem. Res.* **1998**, *37*, 3159−3168.
(18) Yim, K. S. Ph.D. Thesis, Stanford University, 2000.
(19) Edwards, D. A.; Wasan, D. T.; Brenner, H. *Interfacial Transport Processes and Rheology*; Butterworth-Heinemann: Boston, MA, 1991; Chapter 4.
(20) Miller, R.; Wustneck, R.; Kragel, J.; Kretzschmar, G. *Colloid Surf. A* **1996**, *111*, 75−118.
(21) Johnson, D. O.; Stebe, K. J. *Colloid Surf. A* **1996**, *114*, 41−51.
(22) Lucassen, J.; Vandentemple, M. *Chem. Eng. Sci.* **1972**, *27*, 1283−1291.
(23) Saulnier, P.; Boury, F.; Malzert, A.; Heurtault, B.; Ivanova, T.; Cagna, A.; Panaiotov, I.; Proust, J. E. *Langmuir* **2001**, *17*, 8104−8111.
(24) Monroy, F.; Rivillon, S.; Ortega, F.; Rubio, R. G. *J. Chem. Phys.* **2001**, *115*, 530−539.
(25) Monroy, F.; Ortega, F.; Rubio, R. G. *Phys. Rev. E* **1998**, *58*, 7629−7641.
(26) Graham, D. E.; Phillips, M. C. *J. Colloid Interface Sci.* **1980**, *76*, 227−239.
(27) Graham, D. E.; Phillips, M. C. *J. Colloid Interface Sci.* **1980**, *76*, 240−250.
(28) Cardenasvalera, A. E.; Bailey, A. I. *Colloid Surf. A* **1993**, *79*, 115−127.
(29) Brooks, C. F.; Fuller, G. G.; Frank, C. W.; Robertson, C. R. *Langmuir* **1999**, *15*, 2450−2459.
(30) Gaub, H. E.; McConnell, H. M. *J. Phys. Chem.* **1986**, *90*, 6830−6832.
(31) Ghaskadvi, R. S.; Ketterson, J. B.; MacDonald, R. C.; Dutta, P. *Rev. Sci. Instrum.* **1997**, *68*, 1792−1795.
(32) Goodrich, F. C.; Allen, L. H.; Poskanzer, A. *J. Colloid Interface Sci.* **1975**, *52*, 201−212.
(33) Abraham, B. M.; Miyano, K.; Ketterson, J. B.; Xu, S. Q. *Phys. Rev. Lett.* **1983**, *51*, 1975−1978.
(34) Kragel, J.; Siegel, S.; Miller, R.; Born, M.; Schano, K. H. *Colloid Surf. A* **1994**, *91*, 169−180.
(35) Serrien, G.; Geeraerts, G.; Ghosh, L.; Joos, P. *Colloids Surf.* **1992**, *68*, 219−233.
(36) Freer, E. M. Ph.D. Thesis, University of California, in preparation.
(37) Freer, E. M.; Radke, C. J. *J. Adhes.* Submitted for publication.
(38) Rotenberg, Y.; Boruvka, L.; Neumann, A. W. *J. Colloid Interface Sci.* **1983**, *93*, 169−183.
(39) Boyce, J. F.; Schurch, S.; Rotenberg, Y.; Neumann, A. W. *Colloids Surf.* **1984**, *9*, 307−317.
(40) Lunkenheimer, K.; Kretzschmar, G. *Z. Phys. Chem.* **1975**, *256*, 593−605.
(41) Morrison, F. A. *Understanding Rheology*; Oxford University Press: New York, 2001; Chapter 8.
(42) Brown, J. R. *Fed. Proc.* **1976**, *35*, 2141−2144.
(43) Swaisgood, H. E. *Developments in Dairy Chemistry*; Fox, P. F., Ed.; Elsevier Applied Science: London, UK, 1986; pp 1−59.
(44) Dickinson, E.; Horne, D. S.; Phipps, J. S.; Richardson, R. M. *Langmuir* **1993**, *9*, 242−248.
(45) Benjamins, J.; Cagna, A.; LucassenReynders, E. H. *Colloid Surf. A* **1996**, *114*, 245−254.
(46) Lu, J. R.; Su, T. J.; Thomas, R. K. *J. Colloid Interface Sci.* **1999**, *213*, 426−437.
(47) Gurkov, T. D.; Russev, S. C.; Danov, K. D.; Ivanov, I. B.; Campbell, B. *Langmuir* **2003**, *19*, 7362−7369.
(48) Williams, A.; Prins, A. *Colloid Surf. A* **1996**, *114*, 267−275.
(49) Lu, J. R.; Su, T. J.; Thomas, R. K.; Penfold, J.; Webster, J. *J. Chem. Soc., Faraday Trans.* **1998**, *94*, 3279−3287.
(50) Svitova, T. F.; Wetherbee, M. J.; Radke, C. J. *J. Colloid Interface Sci.* **2003**, *261*, 170−179.
(51) Tupy, M. J. Ph.D. Thesis, University of California, 1998.
(52) Graham, D. E.; Phillips, M. C. *J. Colloid Interface Sci.* **1979**, *70*, 415−426.
(53) Martin, A. H.; Meinders, M. B. J.; Bos, M. A.; Stuart, M. A. C.; van Vliet, T. *Langmuir* **2003**, *19*, 2922−2928.
(54) Mellema, M.; Clark, D. C.; Husband, F. A.; Mackie, A. R. *Langmuir* **1998**, *14*, 1753−1758.
(55) Nino, M. R. R.; Sanchez, C. C.; Patino, J. M. R. *Colloid Surf. B* **1999**, *12*, 161−173.
(56) Harzallah, B.; Aguie-Beghin, V.; Douillard, R.; Bosio, L. *Int. J. Biol. Macromol.* **1998**, *23*, 73−84.
(57) Patino, J. M. R.; Sanchez, C. C.; Nino, M. R. R. *Food Hydrocolloids* **1999**, *13*, 401−408.
(58) Cicuta, P.; Stancik, E. J.; Fuller, G. G. *Phys. Rev. Lett.* **2003**, *90*.
(59) Fainerman, V. B.; Lucassen-Reynders, E.; Miller, R. *Colloid Surf. A* **1998**, *143*, 141−165.
(60) Fainerman, V. B.; Miller, R.; Wustneck, R. *J. Colloid Interface Sci.* **1996**, *183*, 26−34.
(61) Bauget, F.; Langevin, D.; Lenormand, R. *J. Colloid Interface Sci.* **2001**, *239*, 501−508.
(62) Adamson, A. W.; Gast, A. P. *Physical Chemistry of Surfaces*, 6th ed.; Wiley: New York, 1997; Chapter 4.
(63) Gardner, J. W.; Addison, J. V.; Schechter, R. S. *AICHE J.* **1978**, *24*, 400−406.
(64) Benjamins, J.; Feijter, J. A. D.; Evans, M. T. A.; Graham, D. E.; Phillips, M. C. *Faraday Discuss.* **1975**, 218−229.
(65) Brooks, C. F.; Thiele, J.; Frank, C. W.; O'Brien, D. F.; Knoll, W.; Fuller, G. G.; Robertson, C. R. *Langmuir* **2002**, *18*, 2166−2173.
(66) Naumann, C. A.; Brooks, C. F.; Wiyatno, W.; Knoll, W.; Fuller, G. G.; Frank, C. W. *Macromolecules* **2001**, *34*, 3024−3032.
(67) Graham, D. E.; Phillips, M. C. *J. Colloid Interface Sci.* **1979**, *70*, 427−439.
(68) Naumann, C. A.; Brooks, C. F.; Fuller, G. G.; Lehmann, T.; Ruhe, J.; Knoll, W.; Kuhn, P.; Nuyken, O.; Frank, C. W. *Langmuir* **2001**, *17*, 2801−2806.
(69) Defeijter, J. A.; Benjamins, J. *J. Colloid Interface Sci.* **1982**, *90*, 289−292.
(70) Fainerman, V. B.; Miller, R.; Kovalchuk, V. I. *Langmuir* **2002**, *18*, 7748−7752.
(71) Hambardzumyan, A.; Aguie-Beghin, V.; Panaiotov, I.; Douillard, R. *Langmuir* **2003**, *19*, 72−78.